HHS Public Access

Author manuscript

J Biomech. Author manuscript; available in PMC 2023 September 01.

Published in final edited form as:

J Biomech. 2022 September ; 142: 111238. doi:10.1016/j.jbiomech.2022.111238.

Biochemical and biomechanical characterization of the cervical, thoracic, and lumbar facet joint cartilage in the Yucatan minipig

Rachel C. Nordberg, Ph.D.[1], **Andrew N. Kim, B.S.**[1], **Justin M. Hight, B.S.**[1], **Rithika S. Meka, B.S.**[1], **Benjamin D. Elder, M.D., Ph.D.**[2], **Jerry C. Hu, Ph.D.**[1], **Kyriacos A. Athanasiou, Ph.D.**[1]

[1]Department of Biomedical Engineering, 3131 Engineering Hall, University of California, Irvine, California 92617, USA

[2]Department of Neurosurgery, Orthopedics, and Biomedical Engineering, Mayo Clinic School of Medicine, 200 1st St. SW, Rochester, MN, 55905, USA

Abstract

Facet joint arthrosis causes pain in approximately 7% of the U.S. population, but current treatments are palliative. The objective of this study was to elucidate structure-function relationships and aid in the development of future treatments for the facet joint. This study characterized the articular surfaces of cervical, thoracic, and lumbar facet cartilage from skeletally mature (18–24 mo) Yucatan minipigs. The minipig was selected as the animal model because it is recognized by the U.S. Food and Drug Administration (FDA) and the American Society for Testing and Materials (ASTM) as a translationally relevant model for spine-related indications. It was found that the thoracic facets had a ~2 times higher aspect ratio than lumbar and cervical facets. Lumbar facets had 6.9–9.6 times higher % depth than the cervical and thoracic facets. Aggregate modulus values ranged from 135–262 kPa, much lower than reported aggregate modulus in the human knee (reported to be 530–701 kPa). The tensile Young's modulus values ranged from 6.7–20.3 MPa, with the lumbar superior facet being 304% and 286% higher than the cervical inferior and thoracic superior facets, respectively. Moreover, 3D reconstructions of entire vertebral segments were generated. The results of this study imply that structure-function relationships in the facet cartilage are different from other joint cartilages because biochemical properties are analogous to other articular cartilage sources whereas mechanical properties are not. By providing functional properties and a 3D database of minipig facet geometries, this work may supply design criteria for future facet tissue engineering efforts.

Keywords

Facet joint; zygapophyseal joint; cartilage; biomechanics; structure-function relationships; minipig; characterization

Corresponding Author: Kyriacos A. Athanasiou. athens@uci.edu. 3418 Engineering Hall, Samueli School of Engineering, Dept. of Biomedical Engineering, University of California, Irvine, Irvine, CA 92697-2715.

Introduction

Zygapophyseal joints, also referred to as facet joints, of the spine are highly susceptible to arthrosis, resulting in pain in up to 7% of the U.S. population (Lawrence et al., 2008; Manchikanti et al., 2004). Current clinical interventions are strictly palliative; nerve blocks are used to pinpoint the origin or pain to the facet, and subsequent neurotomies are used to alleviate the pain for up to 9 months at a time (Glaser and Kreiner, 2016). Alternatively, joint fusions can be used to treat severe cases, but these highly invasive procedures result in permanent loss of motion and alter the mechanics of the spine, which can propagate degeneration to adjacent spinal levels in a condition called adjacent segment disease (Park et al., 2004; Sears et al., 2011). Due to the discouragingly short amount of time of relief offered by existing therapies and the undesirable side effects of joint fusions, tissue engineering may offer a motion preserving solution for facet arthrosis by repairing the degenerative cartilage in affected joints (O'Leary et al., 2018).

Although back and neck pain often have multifactorial causes, facet arthropathy is a well-recognized pain generator, though facet degeneration is also prevalent in the asymptomatic population. Based on a study that used controlled comparative local blocks to evaluate chronic, non-specific spine pain in 500 patients, facet-mediated pain accounted for 55% of cervical spine pain, 42% of thoracic spine pain, and 31% of lumbar spine pain (Manchikanti et al., 2004). Interestingly, in a retrospective analysis of 424 patients with chronic spinal pain, it was determined that cervical facet-mediated pain was most prevalent in younger patients (42%), and lowest in the elderly (33%), while it was more variable among age groups in the lumbar spine (Manchikanti et al., 2008). Therefore, facet degeneration is clearly an important source of back and neck pain.

Two facet joints are located at the junction of two vertebrae forming, with the intervertebral disc, what is referred to as the three-joint complex. The facets provide stability to the spine and transmit between 3–25% of the spinal load under normal loading conditions (Yang and King, 1984). Facet degeneration has been observed by itself, in the absence of disc degeneration (Suri et al., 2011). Degeneration in any joint of the three-joint complex can trigger pathological development in the remaining two (O'Leary et al., 2018). For example, the compressive loading on the facets can be increased by up to 70% due to disc narrowing (Adams and Hutton, 1983). Degeneration of the facet can lead to destabilization of the spine, which is associated with the development of conditions such as spondylolisthesis (O'Leary et al., 2018). While there have been a number of studies that have focused on the repair of the intervertebral disc (Francisco et al., 2013; Hudson et al., 2013), to date, only one paper has been published on tissue engineering of the facet (Elder et al., 2010). There is a need for studies that examine the structure-function relationships in the facet to further understand the implications of facet arthrosis and for the development of treatments for patients afflicted with this condition.

To develop a tissue-engineered solution for facet degeneration, functional design criteria must be established through the characterization of native tissue. Targeted studies have examined the functional properties of the canine lumbar facet (Elder et al., 2009) and equine cervical facet (O'Leary et al., 2018). Tribological properties of minipig facet cartilage have

been characterized (Nordberg et al., 2021). Lumbar facet cartilage of the minipig, primate, and rabbit have been characterized in an interspecies comparison study, showing that the minipig and primate models had comparable mechanical properties (O'Leary et al., 2017). Although the minipig is a quadruped, porcine models are recommended by ASTM and the FDA for studying spine-related indications (ASTM, 2015; FDA, 2000). Because the minipig is a more widely available model for translational studies than the primate, it is desirable to further develop the minipig as a model for tissue-engineered facet replacements by conducting an in-depth characterization.

In the current study, a comprehensive characterization of the minipig facets of the three anatomical regions of the spine (i.e., cervical, thoracic, and lumbar) was conducted. Given that the mechanical environment plays a significant role in the regulation of cartilage homeostasis (Guilak, 2011), mechanical characteristics of facet cartilage were examined in both compression and tension in addition to biochemical and histological characterization. There is a growing interest in developing validated computational models of the facet joint, as recently reviewed (Mengoni, 2021). Critical to the development of accurate finite element models of the facet is the input of both material properties and geometries and, therefore, in addition to functional characterization data, three-dimensional reconstructions of the joints were generated. Data provided by this study can be used to model facet biomechanics *in situ* and guide the development of treatments for facet arthrosis that will help alleviate pain while maintaining joint function.

Methods

Level selection and notation

This study utilized facets isolated from levels of clinical relevance in the human. Human patients are prone to facet degeneration in the cervical and lumbar regions, specifically, C6-C7 in the cervical spine (Kim et al., 2019) and L4-L5 in the lumbar spine (i.e., the level most proximal to the sacrum plus one) (Fujiwara et al., 2000; Kalichman et al., 2008; Vogt et al., 2003). Minipigs have the same number of cervical vertebrae as the human, and, thus, the C6-C7 facet was characterized in the minipig. The number of lumbar vertebrae in a pig varies from animal to animal; the level most proximal to the sacrum plus one was selected for examination, which is either L4-L5 or L5-L6 in the minipig. Thoracic facets are relatively unstudied for the human, and, thus, it is unclear which level would be of the greatest clinical relevance. The T4-T5 level of the minipig was selected because it was within the region of the spine restricted by the ribcage, and, thus, this level has functional demands distinct from the cervical and lumbar facets. 3D reconstructions were of the C5, C6, T4, T5, L5, and L6 vertebrae from both minipigs and were generated via 3D laser scanning as described in the 3D laser scanning and reconstruction methods section. Histology was performed on the levels characterized by quantitative analysis (i.e., C6-C7, T4-T5, and L5-L6 or L4-L5) and from adjacent spine levels (i.e., C5-C6, T5-T6, L4-L5 or L3-L4).

Specimen preparation

Spines were obtained from eight skeletally mature (18–24 mo) Yucatan minipigs sacrificed for reasons unrelated to the current study. In accordance with NIH policy on sex as a biologic variable (Clayton, 2016), tissue was collected from both male and female minipigs (4 each). Spines were dissected to provide access to the facets (Figure 1). Both superior and inferior articular surfaces were utilized for morphometric and functional characterization. Using standard terminology, cartilage from the inferior articular process was termed inferior and the cartilage from the superior articular process was termed superior (e.g., in the L5-L6 joint, the inferior surface is located on the inferior articular process of the L5 vertebral body, and the superior surface is located on the superior articular process of the L6 vertebral body). The facets were imaged using an Olympus TG-5 digital camera (Olympus Corporation, Tokyo, Japan), and dimensions of the facet length (cranial/caudal axis) and width (perpendicular to the length) were taken via ImageJ analysis (n=6 per group). Samples were frozen in gauze soaked in phosphate-buffered saline (PBS)-containing protease inhibitors 10 mmol/L N-ethylmaleimide and 1 mmol/L phenylmethylsulfonyl fluoride (Sigma-Aldrich, St. Louis, MO) at −20°C until testing.

Histology

Samples were processed for biochemistry and mechanical testing (selecting either right facets or left facets in a randomized fashion), and contralateral facets were fixed for histology in 10% neutral buffered formalin. Specimens were decalcified in a 20% ethylenediamine tetraacetic acid (EDTA) solution before processing and sectioned at a thickness of 6μm. Sections were then stained via hematoxylin and eosin, Safranin O/fast green, and picrosirius red to visualize tissue organization, glycosaminoglycan (GAG) content, and collagen content, respectively.

Biochemistry

The biochemical composition of the facets was assessed to quantify the DNA, collagen, and GAG content. Percent hydration was determined by measuring tissue weight before and after lyophilization. Tissue samples were digested in papain (Sigma-Aldrich, St. Louis, MO) at a concentration of 125 μg/ml for 18 hr at 60°C. DNA was measured using a PicoGreen Assay kit (Life Technologies, Carlsbad, CA). GAG content was assessed via a Blyscan Glycosaminoglycan Assay kit (Biocolor, Newtownabbey, Northern Ireland). Total collagen content was assessed using a chloramine-T hydroxyproline assay, as previously described (Cissell et al., 2017).

Mechanical testing

To determine tensile characteristics of the facets, samples were subjected to uniaxial tensile testing. Cartilage strips were removed from the facet with the long axis in the cranial/caudal axis of the joint. Strips were cut into dog bone shapes and imaged to obtain dimensions via ImageJ analysis. Using an Instron Model 5565, samples were pulled at a constant strain rate of 1% per second until they failed. Young’s modulus, ultimate tensile stress (UTS), and strain at failure were calculated in MATLAB.

Compression testing was performed using a creep indentation device, as described previously (Athanasiou et al., 1994). The cartilage was tested on the bone. The sample was submerged in PBS, and a 1mm flat and porous indenter tip was used to first apply a tare load. Then a test load of 2.2g (0.02 N) was applied, and the deformation was recorded over time. A linear biphasic model and finite element optimization were used to calculate the aggregate modulus, shear modulus, and permeability, as previously described (Athanasiou et al., 1995).

3D laser scanning and reconstructions

Two spines (one male, one female) were reserved for generating digital reconstructions of vertebrae. Vertebrae were disarticulated, fixed in 10% buffered formalin, and placed in 3% hydrogen peroxide. The vertebrae were then scanned with the ATOS Core 200 laser scanner using the corresponding GOM scan software (ZEISS, Oberkochen, Germany), which generates high-precision 3D reconstructions with 0.08mm point spacing. Files were exported as .stl files, which were subsequently processed using Geomagic Design X (Artec 3D, Luxembourg, Luxembourg) using the mesh build-up wizard and rewrap function. Any remaining artifacts in the mesh were smoothened in Meshmixer (Autodesk Inc., San Rafael, CA).

Statistics

All numerical data consist of an average of n=5–6 samples. Data are presented as the average ± standard deviation. Statistical analyses were conducted in Prism 8 (GraphPad Software, San Diego, CA). Analysis of variance (ANOVA) tests were used to analyze data sets with Tukey's *post hoc* testing at $p<0.05$.

Results

Gross morphology

To characterize the structure of minipig vertebrae and corresponding facets, laser scans of entire vertebral bodies were obtained (Figure 2). 3D reconstructions of vertebrae isolated from a male and female minipig were generated and are available for download as supplemental files (see linked Mendeley Data files at https://data.mendeley.com/datasets/7s6k7vftrk/draft?a=8ee77828-24f7-4e7e-b96f-fa2d6b4dbbdd). Lumbar facets in the minipig exhibited distinct curvature, which agreed with previously reported morphological data (O'Leary et al., 2017). Thoracic and cervical facets did not exhibit curvature.

Facet dimensions were quantified from ImageJ analysis of samples used for functional testing. Curvature was quantified using a ratio of curvature depth to width as previously described (O'Leary et al., 2018) and is referred to as % depth (Figure 3A). Width varied significantly, being narrower in the thoracic region (Figure 3B). Additionally, % depth was significantly higher in the lumbar facets than in either the cervical or thoracic facets. When analyzed via two-way ANOVA, the effect of surface (i.e., inferior vs. superior) was not significant in any morphologic data set. However, the effect of location (i.e., cervical vs. thoracic vs. lumbar) was significant in the width ($p<0.0001$), aspect ratio ($p<0.0001$), and % depth ($p<0.0001$) data sets.

Histology

Histological staining revealed that the tissue architecture resembled that of typical hyaline articular cartilage (Figure 4). Columnar organization of chondrocytes in the deep zone and tidemarks were observed. Superficial chondrocytes were smaller and flatter, as is characteristic of articular cartilage. Moreover, GAG and collagen staining was observed in all locations with similar staining intensity. Altogether, histological staining was relatively consistent across all facet locations.

Biochemistry

Biochemical content was evaluated on each facet surface (Figure 5). Percent hydration was similar among groups with values of 73±3%, 74±2%, 72±4%, 70±2%, 71±5%, 72±3% for the cervical superior, cervical inferior, thoracic superior, thoracic inferior, lumbar superior, and lumbar inferior, respectively. In the same order, the average percent DNA per dry weight was 0.15±0.08%, 0.13±0.04%, 0.14±0.05%, 0.11±0.06%, 0.15±0.09%, average percent GAG per dry weight was 15.6±11.0%, 10.4±10.9%, 9.0±5.1%, 16.4±9.9%, 14.9±17.5%, 13.5±11.4%, and average percent collagen per dry weight was 64.8±22.5%, 72.6±22.4%, 82.1±9.7%, 70.3±20.0%, 69.5±16.7%, and 65.0±14.7%. No significant differences were observed in the biochemical content of facet cartilage isolated from each anatomical location.

Mechanical testing

Tensile and compressive properties of facets were evaluated (Figure 6). In terms of tensile properties, the Young's modulus of the facet cartilage was 9.2±8.9 MPa, 6.7±3.3 MPa, 7.1±3.8 MPa, 13.4±7.7 MPa, 14.0±4.5 MPa, 20.3±11.0 MPa for the cervical superior, cervical inferior, thoracic superior, thoracic inferior, lumbar superior, and lumbar inferior, respectively. The Young's modulus of the lumbar inferior facet cartilage was significantly higher than the Young's modulus of the cervical inferior ($p=0.03$) or thoracic superior ($p=0.03$) facets. The ultimate tensile stress of the facet cartilage was 8.2±5.2 MPa, 6.4±3.3 MPa, 5.7±3.4 MPa, 11.5±7.0 MPa, 8.6±2.6 MPa, 12.9±5.0 MPa for the cervical superior, cervical inferior, thoracic superior, thoracic inferior, lumbar superior, and lumbar inferior, respectively. Reported in the same order the ultimate tensile strain was 1.3±0.4, 1.6±1.1, 1.0±0.3, 1.4±0.6, 0.9±0.3, and 1.0±0.3. No significant differences were found among groups in the ultimate tensile stress or ultimate tensile strain.

In terms of compressive properties, no significant differences were observed in any of the properties examined. The aggregate modulus of the facet cartilage was 219±106 kPa cervical superior, 243±50 kPa cervical inferior, 262±66 kPa thoracic superior, 135±50 kPa thoracic inferior, 196±75 kPa lumbar superior, and 207±85 kPa lumbar inferior. Reported in the same order, permeability values were 81±71 $10^{-15}m^4/Ns$, 49±53 $10^{-15}m^4/Ns$, 22±11 $10^{15}m^4/Ns$, 42±21 $10^{-15}m^4/Ns$, 26±23 $10^{-15}m^4/Ns$, and 27±12 $10^{-15}m^4/Ns$. Similarly, shear modulus values were 68±29 kPa, 96±31 kPa, 102±30 kPa, 55±16 kPa, 78±25 kPa, and 92±47 kPa.

When analyzed via two-way ANOVA, the effect of surface (i.e., inferior vs. superior) was not significant in any mechanical testing data set. However, the effect of location (i.e., cervical vs. thoracic vs. lumbar) was significant in the Young's modulus data set ($p=0.01$).

Data were examined with respect to sex of the minipig. With n=3 per sex, no sex-related differences were observed. *Post hoc* power analysis of the aggregate modulus of male vs. female samples in the cervical inferior facet revealed an n=448 minipigs would be required to detect a significant difference between males and females. *Post hoc* power analysis of other functional properties showed that similarly high sample sizes are needed to detect sex-related differences, therefore sex does not appear to greatly influence the functional properties of facet cartilage.

Discussion

Toward the development of tissue-engineered facets, the objective of this study was to quantitatively characterize morphometric and functional properties of facet cartilage isolated from the three major spinal regions (i.e., cervical, thoracic, and lumbar), using the minipig as a model. It was found that minipig facets have morphometric characteristics that vary significantly among regions of the spine, with greater curvature observed in the lumbar facets than either the cervical or thoracic facets. While properties such as biochemical content and aggregate modulus of facet cartilage remained relatively constant throughout the regions of the spine, the Young's modulus of cartilage isolated from the inferior lumbar facets was significantly higher than the inferior cervical or superior thoracic facet cartilage. Understanding these differences will allow researchers to define design criteria for tissue-engineered facet replacements and to identify levels most suitable for preclinical animal models of the facet joint.

The biochemical content of minipig facet cartilage was relatively constant across all examined facet surfaces and corresponded to values previously reported in literature. For example, in the canine lumbar facets, collagen/dry weight (DW) was reported to range from 64.8–65.5%, (Elder et al., 2009) which is comparable to the range of 64.8–82.1% observed in this study. With respect to articular cartilage, a characterization of ovine articular cartilage yielded collagen/DW values of 63.6–81.7% (Huwe et al., 2018). Thus, in terms of total collagen content, facet cartilage has similar properties to previously reported values of articular cartilage. Similarly, the GAG/DW range of the canine lumbar facet was reported to be 13.8–16.1% (Elder et al., 2009), which was comparable to the range of 9.0–16.4% observed in this study. In ovine articular cartilage the GAG/DW content was reported to be similar to this range but trended slightly higher at 13.6–19.0% (Huwe et al., 2018), Histological staining was typical to what is seen in other articular cartilages. Thus, biochemically and histologically facet cartilage exhibits the previously observed characteristics of articular cartilage.

Mechanical properties of the facet cartilage differ from other articular cartilage sources; notably, ultimate tensile strain and aggregate modulus values are distinct from those of articular cartilage of the knee. Specifically, we report ultimate tensile strain to range from 0.9–1.6 while articular cartilage isolated from bovine knees has been reported to fail at approximately 0.3 (Sasazaki et al., 2006). Despite the elevated strain at failure observed in these samples, other tensile properties were on par with native tissue. The highest Young's modulus value was observed in the inferior lumbar region at 20.2 MPa and the lowest Young's modulus values were observed in the cervical inferior and thoracic superior

facets (6.7 MPa and 7.1 MPa, respectively). The elevated tensile properties observed in the lumbar facet may be due to the curvature of the lumbar facet restricting range of motion except in flexion/extension, which may have resulted in anisotropic tissue alignment. The tensile modulus values of facet cartilage were similar to those of articular cartilage in the sheep, which were reported to range from 5.8–28.5 MPa (Huwe et al., 2018). Similar trends were observed with ultimate tensile stress, with facet cartilage ranging from 5.7–12.9 MPa and sheep knee cartilage ranging from 3.3–17.3 MPa (Huwe et al., 2018). In terms of compressive properties, the aggregate modulus of the minipig facet was lower than previously reported values in articular cartilage. The aggregate modulus values of the distal femoral cartilage have been reported to range from 530–701 kPa in the human, 472– 899 kPa in the cow, 555–603 kPa in the dog, 522–815 kPa in the monkey, and 516–741 kPa in the rabbit (Athanasiou et al., 1991). In the sheep, the aggregate modulus of articular cartilage of the knee ranged from 183–364 kPa (Huwe et al., 2018). Because aggregate modulus values in the current study ranged from 135–262 kPa, the compressive properties of the minipig facet cartilage appear to be lower than most other articular cartilage sources. Therefore, although biochemical properties are analogous to other articular cartilage sources mechanical properties are not, implying that structure-function relationships are altered within the facet joint.

This study supplies a total of 12 reconstructed Yucatan minipig vertebrae, which have several potential applications. First, toward the development of anatomically shaped facet implants, these models provide the first published porcine 3D reconstructions that can be utilized to guide facet-shaped computer-aided design and manufacturing. Second, there has been an interest in studying the biomechanics of the spine and facet with finite element analysis, as recently reviewed (Mengoni, 2021; Wu et al., 2021). The provided reconstructions, in conjunction with the other functional properties reported in this study, can assist with the generation of detailed models of the three-joint complex to study spine biomechanics. Finally, because porcine models can be used for preclinical studies in the spine (ASTM, 2015; FDA, 2000), this study's 3D reconstruction of 12 minipig vertebrae can help guide surgical planning in large animal studies.

The Yucatan minipig model was used in this characterization as a clinically relevant animal model. In recent years, porcine models have been used increasingly to study musculoskeletal biomechanics and tissue engineering (Cone et al., 2017). With regard to the spine, selecting an appropriate model has been acknowledged by the FDA to be challenging (FDA, 2000). However, minipig models have been recognized and accepted for spine-related research by both ASTM and the FDA (ASTM, 2015; FDA, 2000). Moreover, it has been reported that functional properties of the minipig and primate facet cartilage were similar (O'Leary et al., 2017). Therefore, the minipig may be a front runner in terms of potential non-primate animal models for facet research. Several limitations of this model should be considered moving forward. For example, the porcine spine has been reported to have a lower range of axial rotation and flexion/extension than the human (Wilke et al., 2011). Additionally, human and minipig lumbar facets have been reported to have different radii of curvature (O'Leary et al., 2017). However, as reported here, the minipig cervical and thoracic facets do not display the same curvature as the lumbar facets and therefore may be more relevant to the human anatomy. Moreover, only morphologically healthy facet tissues were observed

in this study. There is considerable interest in facet pathology due to the high incidence of degeneration in human facets (O'Leary et al., 2017; Suri et al., 2013), afflicting 57% of the population by the age of 30 (Eubanks et al., 2007). As the current study used skeletally mature minipigs that correspond in age to late-adolescent humans (Cone et al., 2017), future studies in older minipigs are required to determine if facet pathology can be observed in this model.

Facet tissue engineering may be achievable using techniques that have already been developed. Compared to the knee, the facet is subjected to relatively low stresses. For example, in humans, the facet joint may experience up to approximately 120 N of contact force with a surface area as low as 0.69 cm^2 (O'Leary et al., 2018). Thus, the highest stress expected in the lumbar facet is approximately 1.7 MPa, which is almost one order of magnitude lower than compressive stresses in the knee which reach approximately 14 MPa (Thambyah et al., 2005). The lower expected loading requirements correspond to the lower aggregate modulus values reported in this study. It has been previously reported that self-assembled neocartilage can be generated with a ~400 kPa aggregate modulus and ~8 MPa tensile Young's modulus (Lee et al., 2017; Salinas et al., 2020). Composite scaffolds composed of a 3D woven polymer yarn consolidated with a chondrocyte–hydrogel mixture have been reported to have aggregate modulus values ranging from 140–1200 kPa, depending on the hydrogel formulation used (Liao et al., 2013; Moutos et al., 2007). High-density collagen hydrogels have also been generated with mechanical properties that recapitulate those of facet cartilage, reporting aggregate modulus values in excess of 300 kPa (Cohen et al., 2016; Middendorf et al., 2017). In the current study, it was shown that the inferior cervical facet, for example, had an aggregate modulus of 243 kPa and a tensile Young's modulus of 6.7 MPa, which is obtainable with currently available technologies. In terms of total joint replacement, it has been reported that self-assembled constructs up to 9.3 cm^2 in surface area can be generated (Huang et al., 2018). This surface area is much larger than the surface area of human facets, which range from 0.69–2.12 cm^2 (O'Leary et al., 2018). The cervical and thoracic facets used in this study were relatively flat, which would reduce complications in manufacturing an anatomic geometry. Therefore, the development of tissue-engineered facets may be imminently feasible because native facet functional properties and geometries can be replicated with existing tissue engineering methods.

Conclusions

In conclusion, this study will aid the development of therapies to treat facet degeneration by providing functional characterization data. This will contribute to a growing body of literature that aims to elucidate the structure-function relationships of the facet, and further develop the minipig as a large animal model for facet tissue repair. These data will allow researchers to generate detailed finite element models to elucidate spine biomechanics. Moreover, these data can serve as design criteria for future tissue engineering work and, therefore, contribute to the development of tissue-engineered approaches to treat facet arthrosis.

Acknowledgments

This study was supported by two grants from the NIH (Grant # R01 AR067821 and R01 AR078389). This work was also supported by NIH TL1 TR001415 (RCN). The content is solely the responsibility of the authors and does not necessarily represent the official views of the NIH. Drs. Athanasiou and Hu have an equity interest in Cartilage, Inc. Their relationship with Cartilage, Inc. has been reviewed and approved by the University of California, Irvine in accordance with its conflict-of-interest policies.

References

Adams MA, Hutton WC, 1983. The mechanical function of the lumbar apophyseal joints. Spine (Phila. Pa. 1976). 8, 327–330. 10.1097/00007632-198304000-00017 [PubMed: 6623200]

ASTM, 2015. Standard Guide for Pre-clinical in vivo Evaluation of Spinal Fusion 1. Astm. 10.1520/F2884

Athanasiou KA, Agarwal A, Dzida FJ, 1994. Comparative study of the intrinsic mechanical properties of the human acetabular and femoral head cartilage. J Orthop Res 12, 340–349. 10.1002/jor.1100120306 [PubMed: 8207587]

Athanasiou KA, Agarwal A, Muffoletto A, Dzida FJ, Constantinides G, Clem M, 1995. Biomechanical properties of hip cartilage in experimental animal models. Clin. Orthop. Relat. Res 254–66.

Athanasiou KA, Rosenwasser MP, Buckwalter JA, Malinin TI, Mow VC, 1991. Interspecies comparisons of in situ intrinsic mechanical properties of distal femoral cartilage. J. Orthop. Res 9, 330–340. 10.1002/jor.1100090304 [PubMed: 2010837]

Cissell DD, Link JM, Hu JC, Athanasiou KA, 2017. A Modified Hydroxyproline Assay Based on Hydrochloric Acid in Ehrlich's Solution Accurately Measures Tissue Collagen Content. Tissue Eng Part C Methods 23, 243–250. 10.1089/ten.tec.2017.0018 [PubMed: 28406755]

Clayton JA, 2016. Studying both sexes: A guiding principle for biomedicine. FASEB J. 30, 519–524. 10.1096/fj.15-279554 [PubMed: 26514164]

Cohen BP, Hooper RC, Puetzer JL, Nordberg R, Asanbe O, Hernandez KA, Spector JA, Bonassar LJ, 2016. Long-Term Morphological and Microarchitectural Stability of Tissue-Engineered, Patient-Specific Auricles In Vivo. Tissue Eng. A 22, 461–468. 10.1089/ten.TEA.2015.0323 [doi]

Cone SG, Warren PB, Fisher MB, 2017. Rise of the Pigs: Utilization of the Porcine Model to Study Musculoskeletal Biomechanics and Tissue Engineering During Skeletal Growth. Tissue Eng. Part C Methods 23, 763–780. 10.1089/ten.tec.2017.0227 [PubMed: 28726574]

Elder B, 2009. Biomechanical, biochemical, and histological characterization of canine lumbar facet joint cartilage. J. Neurosurg. Spine 10, 623–628. 10.3171/2009.2.SPINE08818 [PubMed: 19558298]

Elder BD, Kim DH, Athanasiou KA, 2010. Developing an articular cartilage decellularization process toward facet joint cartilage replacement. Neurosurgery 66, 722–7; discussion 727. 10.1227/01.neu.0000367616.49291.9f [PubMed: 20305493]

Eubanks JD, Lee MJ, Cassinelli E, Ahn NU, 2007. Prevalence of lumbar facet arthrosis and its relationship to age, sex, and race: an anatomic study of cadaveric specimens. Spine (Phila Pa 1976) 32, 2058–2062. 10.1097/BRS.0b013e318145a3a9 [PubMed: 17762805]

FDA, 2000. Guidance for Industry and/or FDA Reviewers/Staff Guidance Document for the Preparation of IDEs for Spinal Systems.

Francisco AT, Mancino RJ, Bowles RD, Brunger JM, Tainter DM, Chen Y. Te, Richardson WJ, Guilak F, Setton LA, 2013. Injectable laminin-functionalized hydrogel for nucleus pulposus regeneration. Biomaterials 34, 7381–7388. 10.1016/J.BIOMATERIALS.2013.06.038 [PubMed: 23849345]

Fujiwara A, Lim TH, An HS, Tanaka N, Jeon CH, Andersson GB, Haughton VM, 2000. The effect of disc degeneration and facet joint osteoarthritis on the segmental flexibility of the lumbar spine. Spine (Phila Pa 1976) 25, 3036–3044. [PubMed: 11145815]

Glaser J, Kreiner S, 2016. Facet Joint Interventions. North Am Spine Soc.

Guilak F, 2011. Biomechanical factors in osteoarthritis. Best Pract. Res. Clin. Rheumatol 25, 815. 10.1016/J.BERH.2011.11.013 [PubMed: 22265263]

Huang BJ, Brown WE, Keown T, Hu JC, Athanasiou KA, 2018. Overcoming Challenges in Engineering Large, Scaffold-Free Neocartilage with Functional Properties. Tissue Eng. Part A 10.1089/ten.TEA.2017.0495

Hudson KD, Alimi M, Grunert P, Härtl R, Bonassar LJ, 2013. Recent advances in biological therapies for disc degeneration: tissue engineering of the annulus fibrosus, nucleus pulposus and whole intervertebral discs. Curr. Opin. Biotechnol 24, 872–879. 10.1016/J.COPBIO.2013.04.012 [PubMed: 23773764]

Huwe LW, Brown WE, Hu JC, Athanasiou KA, 2018. Characterization of costal cartilage and its suitability as a cell source for articular cartilage tissue engineering. J. Tissue Eng. Regen. Med 12, 1163–1176. 10.1002/term.2630

Kalichman L, Li L, Kim D, Guermazi A, Berkin V, O'Donnell CJ, Hoffmann U, Cole R, Hunter DJ, 2008. Facet joint osteoarthritis and low back pain in the community-based population. Spine (Phila. Pa. 1976). 33, 2560. [PubMed: 18923337]

Kim JH, Sharan A, Cho W, Emam M, Hagen M, Kim SY, 2019. The prevalence of asymptomatic cervical and lumbar facet arthropathy: A computed tomography study. Asian Spine J. 13, 417–422. 10.31616/asj.2018.0235 [PubMed: 30744307]

Lawrence RC, Felson DT, Helmick CG, Arnold LM, Choi H, Deyo RA, Gabriel S, Hirsch R, Hochberg MC, Hunder GG, Jordan JM, Katz JN, Kremers HM, Wolfe F, 2008. Estimates of the prevalence of arthritis and other rheumatic conditions in the United States. Part II. Arthritis Rheum. 58, 26–35. 10.1002/art.23176 [PubMed: 18163497]

Lee JK, Huwe LW, Paschos N, Aryaei A, Gegg CA, Hu JC, Athanasiou KA, 2017. Tension stimulation drives tissue formation in scaffold-free systems. Nat. Mater 16, 864–873. 10.1038/nmat4917 [PubMed: 28604717]

Liao IC, Moutos FT, Estes BT, Zhao X, Guilak F, 2013. Composite three-dimensional woven scaffolds with interpenetrating network hydrogels to create functional synthetic articular cartilage. Adv. Funct. Mater 23, 5833–5839. 10.1002/ADFM.201300483 [PubMed: 24578679]

Manchikanti L, Boswell MV, Singh V, Pampati V, Damron KS, Beyer CD, 2004. Prevalence of facet joint pain in chronic spinal pain of cervical, thoracic, and lumbar regions. BMC Musculoskelet. Disord. 5, 15. 10.1186/1471-2474-5-15

Manchikanti L, Manchikanti KN, Cash KA, Singh V, Giordano J, 2008. Age-related prevalence of facet-joint involvement in chronic neck and low back pain. Pain Physician 11, 67–75. [PubMed: 18196171]

Mengoni M, 2021. Biomechanical modelling of the facet joints: a review of methods and validation processes in finite element analysis. Biomech. Model. Mechanobiol 20, 389–401. 10.1007/s10237-020-01403-7 [PubMed: 33221991]

Middendorf JM, Griffin DJ, Shortkroff S, Dugopolski C, Kennedy S, Siemiatkoski J, Cohen I, Bonassar LJ, 2017. Mechanical properties and structure-function relationships of human chondrocyte-seeded cartilage constructs after in vitro culture. J. Orthop. Res 35, 2298–2306. 10.1002/jor.23535 [PubMed: 28169453]

Moutos FT, Freed LE, Guilak F, 2007. A biomimetic three-dimensional woven composite scaffold for functional tissue engineering of cartilage. Nat. Mater. 2007 62 6, 162–167. 10.1038/nmat1822

Nordberg RC, Espinosa MG, Hu JC, Athanasiou KA, 2021. A Tribological Comparison of Facet Joint, Sacroiliac Joint, and Knee Cartilage in the Yucatan Minipig. Cartilage 19476035211021904. 10.1177/19476035211021906

O'Leary SA, Link JM, Klineberg EO, Hu JC, Athanasiou KA, 2017. Characterization of facet joint cartilage properties in the human and interspecies comparisons. Acta Biomater. 54, 367–376. 10.1016/j.actbio.2017.03.017 [PubMed: 28300721]

O'Leary Siobhan A., Paschos NK, Link JM, Klineberg EO, Hu JC, Athanasiou KA, 2018. Facet Joints of the Spine: Structure–Function Relationships, Problems and Treatments, and the Potential for Regeneration. Annu. Rev. Biomed. Eng 20, 145–170. 10.1146/annurev-bioeng-062117-120924 [PubMed: 29494214]

O'Leary SA, White JL, Hu JC, Athanasiou KA, 2018. Biochemical and biomechanical characterisation of equine cervical facet joint cartilage. Equine Vet. J 10.1111/evj.12845

Park P, Garton HJ, Gala VC, Hoff JT, McGillicuddy JE, 2004. Adjacent Segment Disease after Lumbar or Lumbosacral Fusion: Review of the Literature. Spine (Phila. Pa. 1976). 29, 1938–1944. [PubMed: 15534420]

Salinas EY, Aryaei A, Paschos N, Berson E, Kwon H, Hu JC, Athanasiou KA, 2020. Shear stress induced by fluid flow produces improvements in tissue-engineered cartilage. Biofabrication 12, 045010. 10.1088/1758-5090/ABA412

Sasazaki Y, Shore R, Seedhom BB, 2006. Deformation and failure of cartilage in the tensile mode, J. Anat

Sears WR, Sergides IG, Kazemi N, Smith M, White GJ, Osburg B, 2011. Incidence and prevalence of surgery at segments adjacent to a previous posterior lumbar arthrodesis. Spine J. 11, 11–20. 10.1016/j.spinee.2010.09.026 [PubMed: 21168094]

Suri P, Hunter DJ, Rainville J, Guermazi A, Katz JN, 2013. Presence and extent of severe facet joint osteoarthritis are associated with back pain in older adults. Osteoarthr. Cartil 21, 1199–1206. 10.1016/j.joca.2013.05.013

Suri P, Miyakoshi A, Hunter DJ, Jarvik JG, Rainville J, Guermazi A, Li L, Katz JN, 2011. Does lumbar spinal degeneration begin with the anterior structures? A study of the observed epidemiology in a community-based population. BMC Musculoskelet. Disord. 12. 10.1186/1471-2474-12-202

Thambyah A, Goh JCH, Das De S, 2005. Contact stresses in the knee joint in deep flexion. Med. Eng. Phys 27, 329–335. 10.1016/j.medengphy.2004.09.002 [PubMed: 15823474]

Vogt MT, Rubin DA, Palermo L, Christianson L, Kang JD, Nevitt MC, Cauley JA, 2003. Lumbar spine listhesis in older African American women. Spine J 3, 255–261. [PubMed: 14589183]

Wilke HJ, Geppert J, Kienle A, 2011. Biomechanical in vitro evaluation of the complete porcine spine in comparison with data of the human spine. Eur. Spine J 20, 1859–1868. 10.1007/s00586-011-1822-6 [PubMed: 21674213]

Wu W, Han Z, Hu B, Du C, Xing Z, Zhang C, Gao J, Shan B, Chen C, 2021. A graphical guide for constructing a finite element model of the cervical spine with digital orthopedic software. Ann. Transl. Med 9, 169–169. 10.21037/atm-20-2451 [PubMed: 33569471]

Yang KH, King AI, 1984. Mechanism of facet load transmission as a hypothesis for low-back pain. Spine (Phila Pa 1976) 9, 557–565. 10.1097/00007632-198409000-00005 [PubMed: 6238423]

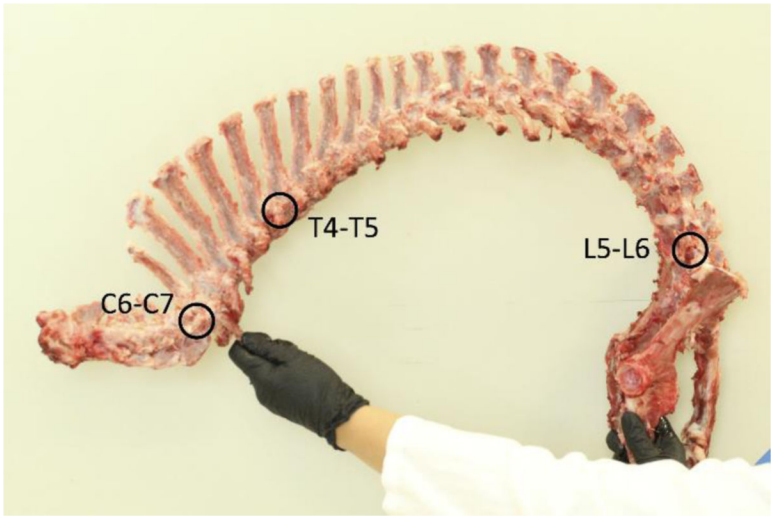

Figure 1:
Entire minipig spine with the location of the C6-C7, T4-T5, and L5-L6 facet joints circled.

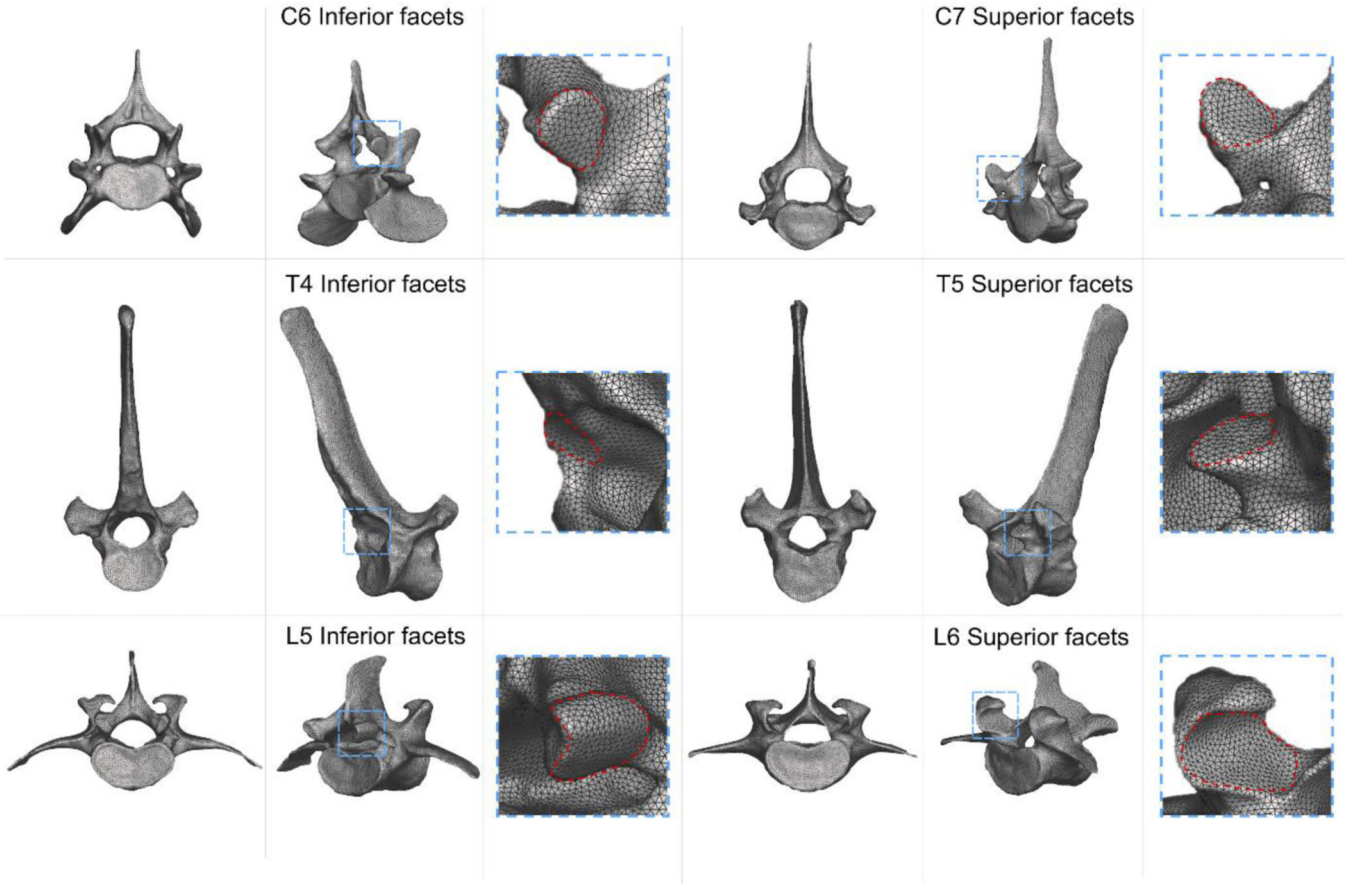

Figure 2:

3D reconstructions of total vertebrae. C6, T4, and L5 vertebrae are oriented so that the caudal side faces forward. C7, T5, and L6 vertebrae are oriented so that the sacral side faces forward. An image of each segment rotated 45° clockwise and a close of up the facet joint are also included. The dashed red line represents the outline of the cartilage surface. Corresponding .stl files are provided via Mendeley data as supplementary downloads.

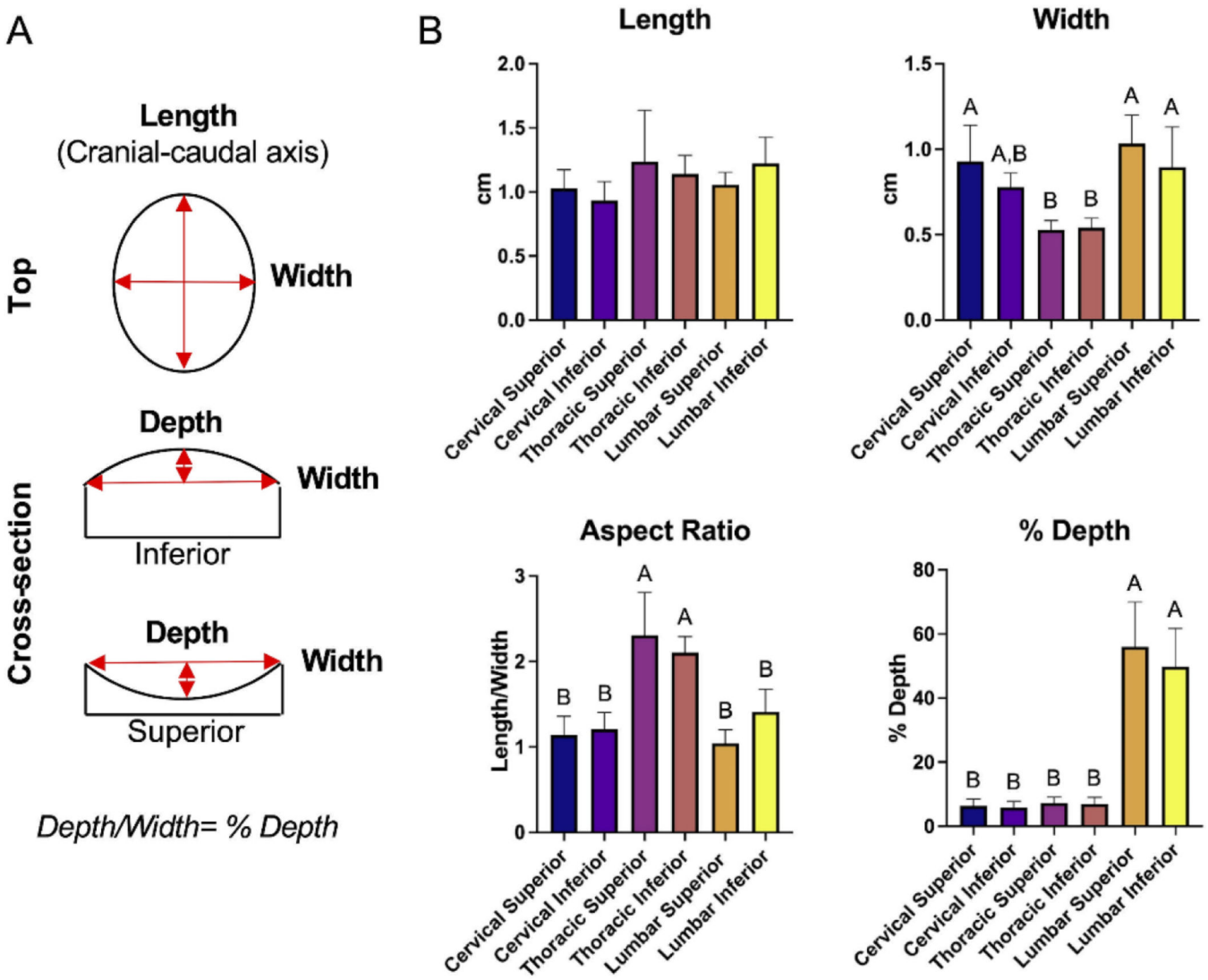

Figure 3:

A. Orientation of morphometric measurements and **B.** morphometric characteristics of minipig facet joints. Values presented are mean+standard deviation for n=5–6. Joints not connected by the same letter are statistically different (p<0.05) from each other.

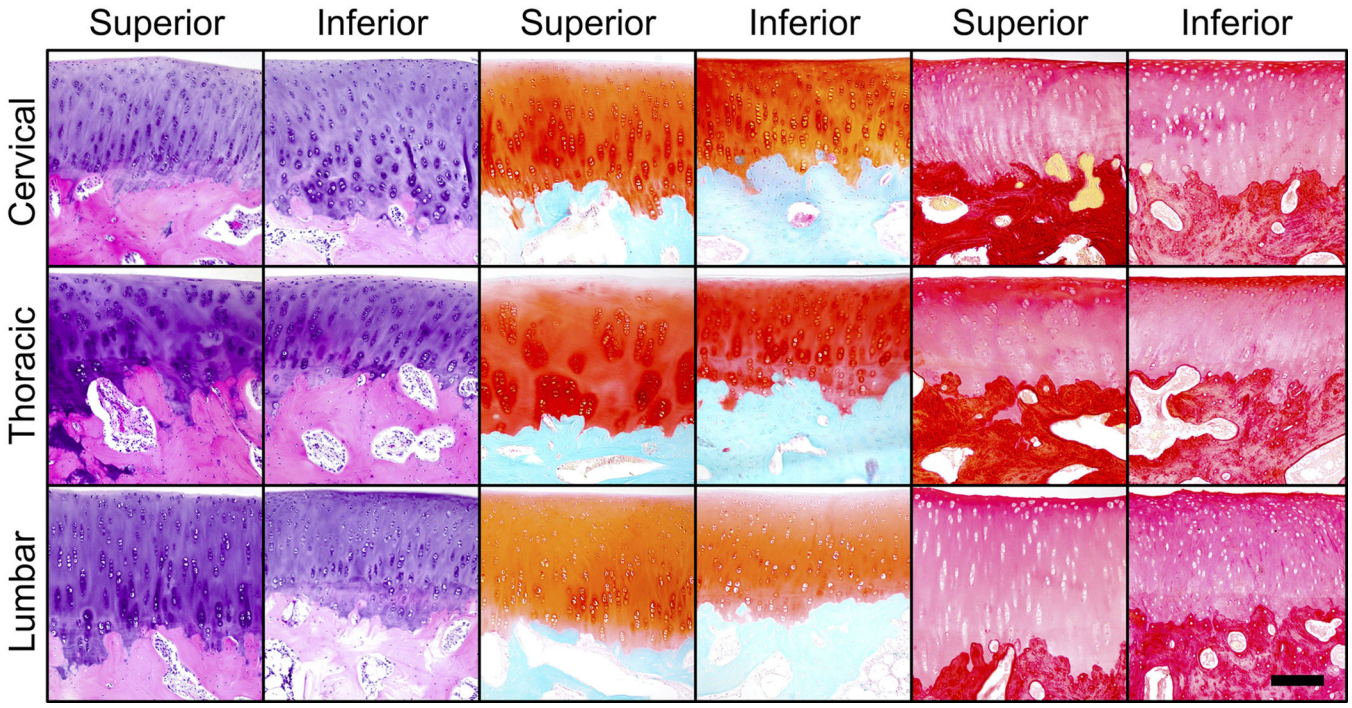

Figure 4:

Histology of minipig facet joints. H&E (left two columns), Safranin-O/fast green (center two columns), and picrosirius red (right two columns) were used to visualize structure, glycosaminoglycans, and collagen content, respectively. Scale bar=200μm.

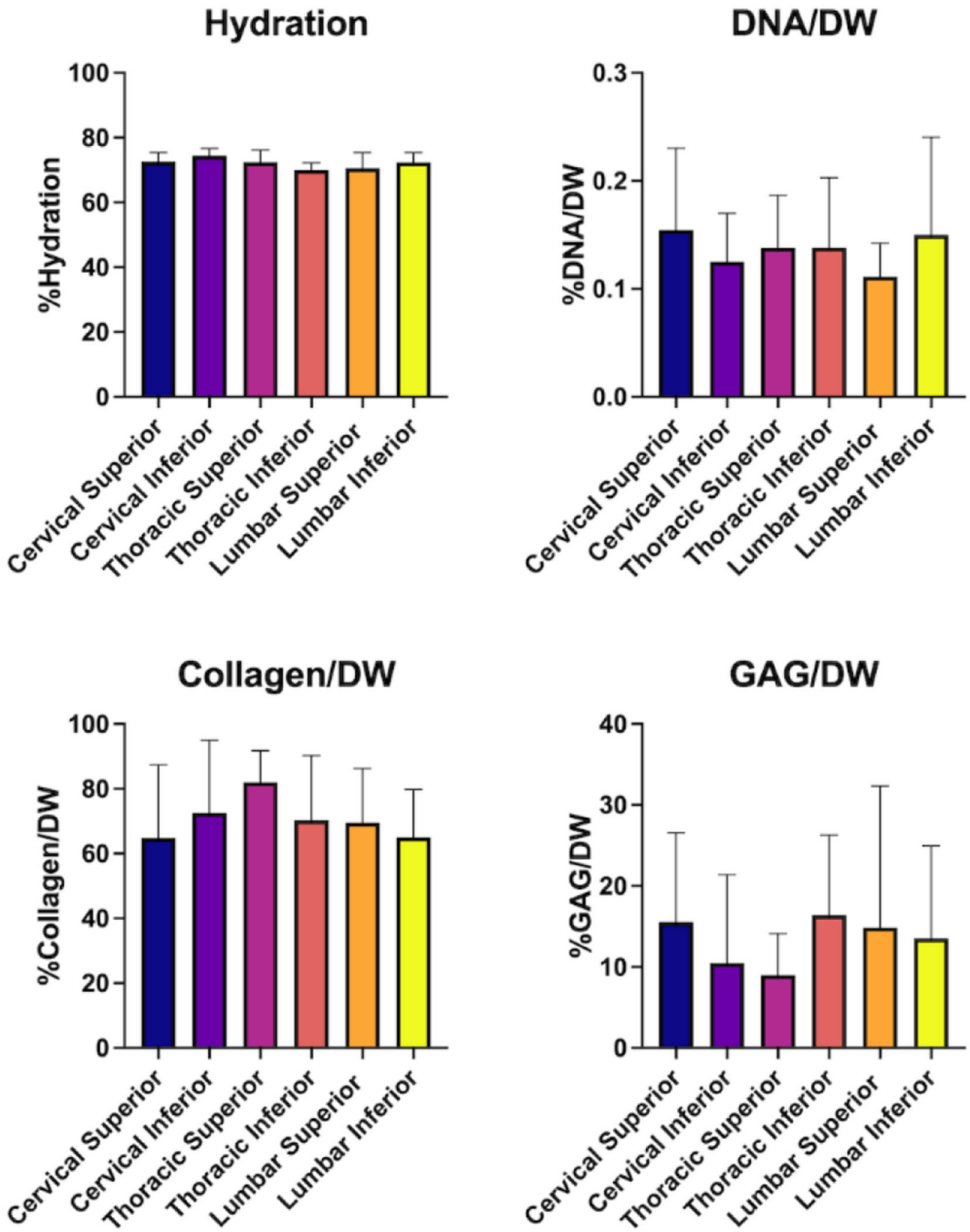

Figure 5:

Biochemical properties of minipig facet joints. Values presented are mean+standard deviation for n=5–6. No statistical significance was observed among joints (p<0.05).

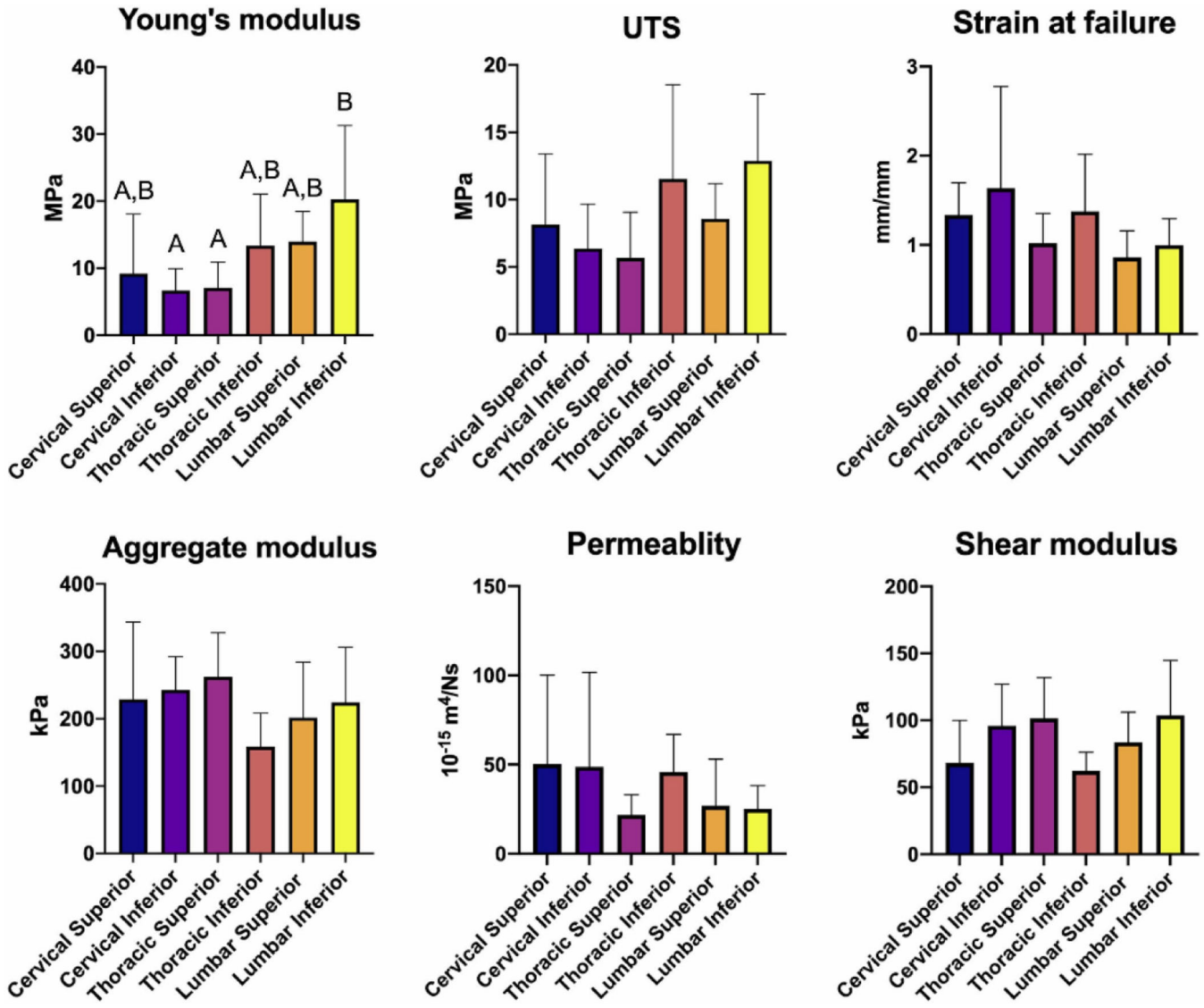

Figure 6:

Biomechanical characteristics of minipig facet joints. Tensile parameters examined were Young's modulus, ultimate tensile stress (UTS), and strain at failure. Compressive properties examined were aggregate modulus, permeability, and shear modulus. Values presented are mean+standard deviation for n=5–6. Joints not connected by the same letter are statistically different from each other (p<0.05).